2016 14th International Conference on Control, Automation, Robotics & Vision
Phuket, Thailand, 13-15th November 2016 (ICARCV 2016)

Formations of Unmanned Micro Aerial Vehicles Led by Migrating Virtual Leader

Martin Saska
Faculty of Electrical Engineering
Czech Technical University in Prague
Email: martin.saska@fel.cvut.cz

Tomas Baca
Faculty of Electrical Engineering
Czech Technical University in Prague
Email: bacatoma@fel.cvut.cz

Daniel Hert
Faculty of Electrical Engineering
Czech Technical University in Prague
Email: hertdani@fel.cvut.cz

***Abstract*—A novel approach for control and motion planning of formations of multiple unmanned micro aerial vehicles (MAVs), also referred to as unmanned aerial vehicles (UAVs) - multirotor helicopters, in cluttered GPS-denied environments is presented in this paper. The proposed method enables autonomously to design complex maneuvers of a compact MAV team in a virtual-leader-follower scheme. The feasibility of obtained results of the motion planning approach and the required stability of the formation is achieved by migrating the virtual leader along a hull surrounding the formation. This enables us to suddenly change formation motion in all directions, independently of actual orientation of the formation.**

I. Introduction

Control and stabilization of MAVs are currently intensively studied research fields due to their high maneuverability and possibility to reach locations hardly accessible by unmanned ground vehicles (UGVs) and by fixed-wing unmanned aerial vehicles (UAVs) that are usually larger and too fast for flying in a straitened environment with obstacles. MAVs are especially appealing for applications in such cluttered workspace since they can fly close to obstacles relatively safely and they enable complex maneuvers in a low speed. The same abilities are required for control of compact closely cooperating multi-MAV teams, where also inter-vehicle coordination of MAVs flying in small relative distances needs to be tackled (see Fig. 1 for examples of our target applications). In addition, the requirements on operation in compact MAV formations in the cluttered workspace close to the obstacles exclude utilization of global navigation satellite systems, such as GPS, with their insufficiently low precision in comparison with required mutual distances between neighbouring MAVs and its low reliability if the signal from satellites is partly or completely disabled by the obstacles.

This paper proposes to solve this problem by a novel motion planning and stabilization approach for control of teams of MAVs flying in compact formations in a cluttered environment without using GPS. The proposed method is focused on key properties required for deployment of the groups of aerial robots in narrow spaces, i.e. efficient motion planning that enables to design autonomously complex maneuvers of the formation and coordination of possibly large MAV groups flying in small relative distances. The required high maneuverability is achieved by inclusion of model predictive control (MPC) and trajectory planning, which is feasible for the MAV formations,

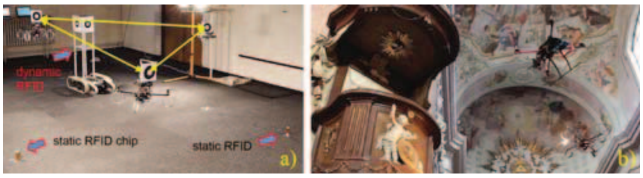

Fig. 1. Examples of practical deployment of parts of the proposed formation flying method. a) Cooperative localization of active RFID chips by a formation of relatively stabilized MAVs of a given shape. b) Documentation of hardly accessible places in historical sites by a formation of MAVs. One MAV carries a camera and its neighbors light sources with possibility to set relative angle between the camera axis and the lights, as it is required by the classical film lighting techniques, such as the three-point lighting approach [3].

into a single optimization process and by employing a concept of a virtual leader migrating along a convex hull surrounding the formation. Such extension of the classical leader-follower (L-F) approach enables to arbitrary change motion direction of the formation enforced by the surrounding environment and by the obstacles, while the requirement given by the L-F technique, in which the leader is always in front of the formation, is satisfied. This enables us to rely on the well-conducted theory of the L-F control technique and to guarantee the stability of the group.

To be able to localize the MAVs in the formation, we rely on an extension of the onboard visual relative localization system using a single camera that we have described in [1], [2]. The extended system, which may be used for real deployment of the theory presented in this paper, enables to estimate relative positions of neighboring robots in the formation using a 360° panoramic view provided by a ring of four onboard monocular cameras and localization patterns carried by each formation member (see Fig. 2). The relative pose is estimated from the detected size of the pattern and its position in the image.

In the presented approach, we will rely on a virtual-leader-follower approach, where all MAVs are considered as followers following a virtual robot in front of the formation. The virtual-leader approach is often used for multi-robot control due to its high robustness (see e.g. [4]), since it is not threatened by a failure of the real leader. In our paper, the motivation for using the virtual leader is different. We take advantage of the possibility to change the virtual leader position relatively to the formation, which enables suddenly change its motion direction while keeping the requirements of the L-F scheme specified

978-1-5090-3549-6/16/$31.00 ©2016 IEEE

Fig. 2. Examples of the outdoor experiments of stabilization of MAV formations using the onboard vison-based relative localization system [1], [2] and picture of the 360° relative localization module.

in [5].

In recent works, the sudden change of the position of the formation leader is usually realized by switching the leadership between different team members to increase the system robustness [6], to enable splitting the team [7], and to reconfigure the formation shape [8]. While all of these works are focused on a study of shape stability of the formation simply following a given path, we will focus on the integration of switching the positions of the virtual leader into the trajectory planning process and on aspects and limitations of deployment of MAVs in close relative distances.

For other examples of recent methods designed for control of MAV formations see [9], [10], [11]. In all of these works, the desired trajectory that is followed by the formation is given or obtained by an external path planning method modified for the formation requirements. An integration of trajectory planning into the formation stabilization process can be found only in [12], where a combination of the L-F approach with a potential field technique is presented. Nevertheless, this algorithm is designed for ground holonomic robots, and it suffers from the usual problems of potential field techniques, such as oscillations near the local extremes, deadlocks in U-shape obstacles and poor performance if avoiding clusters of obstacles. In the presented method, we enable to include a global information about the environment, which is not possible with the method in [12], and to plan complex trajectories in a cluttered environment with obstacles.

As mentioned, we propose to include the ability of global trajectory planning into the MPC scheme within a single optimization process. This approach enables us to integrate the relative-localization constraints, which are crucial for robots deployment in a GPS-denied environment, directly into the formation stabilization process. MPC solutions [13] and [14] have demonstrated that the MPC method can be used for stabilization of a single MAV using an onboard embedded processor. Although these pioneering methods can realize only simple control tasks (such as hovering in ideal windless conditions) due to a short prediction horizon, our solution introduced in [15] enables to control a single MAV using embedded processor and onboard sensors with prediction control horizon longer than 2s, as shown in numerous indoor and outdoor experiments https://youtu.be/lPy7w-GUbw4. Such prediction interval is sufficient for following arbitrary dynamically changing 3D trajectories with the precision and stability required in multi-MAV scenarios (see Fig. 2 for examples of stabilization of MAV formations using the visual relative localization [1], [2]).

This work is built on our achievements in control and stabilization of formations of ground vehicles [16], [17] and heterogeneous teams of ground and aerial robots [18], [19], where the formations were able to follow only simple trajectories without the possibility of changing the motion direction. Moreover, the planning was limited to a plain space due to applied ground robots, which were used for stabilization of the formation relatively to the ground. The possibility of motion direction alternation was introduced in our work [20], [21], which was also designed for the ground (car-like) robots and UGV-UAV teams. Due to the limited motion capabilities of the car-like robots, the formations in [20], [21] may change the motion direction only from the forward motion to the backward motion (i.e. only the 180-degree change of the motion direction). The proposed approach enables to plan maneuvers with the arbitrary change of the motion direction (the change of the motion direction can be done immediately into any angle) of the formation keeping its desired shape in a cluttered workspace. In the proposed MPC approach, the trajectory planning into the desired target, the immediate formation control, and the planning of positions of the virtual follower relatively to the formation are integrated into a single optimization process. Due to this cohesion, the formation can smoothly respond to changes in its vicinity and to consider also the global information about the environment in the control loop. The local control inputs are then optimized not only regarding the short-term obstacle avoidance but also regarding the future movement of the formation.

II. Problem definition

In this paper, a problem of control of an MAV formation of a given shape from its initial position into a spherical target region is tackled. We assume a fixed number N_{MAV} of the MAVs in the formation. It is assumed that the required formation shape, which is specified by curvilinear coordinates p_i, q_i, h_i for each MAV i relatively to the virtual leader, satisfies constraints on the relative localization of all formation members. It means that the maximal distance between any two robots in the formation is shorter than the sensing range of the relative localization system as specified in [2]. Due to the 6-pages limit of this paper, we have to omit description of this curvilinear coordinate system, and we refer to Fig. 4 and to [18] for details. We assume that a finite number of compact obstacles, which are represented in 3D as complex polyhedrons, is located in the workspace. Considering only the polyhedrons, the minimal distance between an obstacle and a convex shape representing the formation can be efficiently obtained by the GilbertJohnsonKeerthi distance algorithm (GJK),

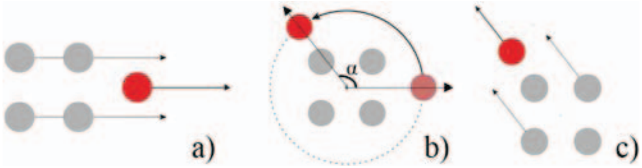

Fig. 3. Migration of the virtual leader to enable sudden change of the flight direction, if the maneuvering in a clustered environment is necessary. Virtual leader - red, followers - grey. a) Flight before the migration. b) Migration of the virtual leader. c) Flight in the new direction.

which is important for fast obstacle avoidance due to its low computational complexity [22]. The obstacles and the target region are represented on a global map, which is shared by all robots. During the mission, new obstacles can be added to the map once they are detected by a follower. A Wi-Fi communication is employed for sharing the map updates and for distribution of desired trajectories to the followers. For localization of MAVs, we assume to rely only on onboard sensors (IMU, PX4flow, and the relative visual localization system [1]) and no external positioning system is available. The global position of the formation in the environment can be obtained relatively imprecisely using any onboard global localization, for example [23].

III. Method description

A. Migrating virtual leader concept

In our method, the virtual "migrating" leader, which is employed to extend the maneuverability of the formation driving approach from [5], is initialized or reinitialized on a 3D convex hull of positions of followers in the direction of further movement of the formation (see Fig. 3). It enables to change the direction of the formation flight suddenly while keeping the virtual leader in front of the formation, which is the main assumption of the L-F approach from [5]. The position of the virtual leader ahead the formation is necessary for the coordination of followers, which required states be computed from the motion history of the virtual leader. If the virtual leader is not positioned in front of all followers, their none-collision flight is not ensured (see Fig. 2 of [24] for example) and the ability of the system to avoid dynamic obstacles is reduced. For simplification of the description of our approach, we use a circumscribed sphere of the 3D hull in Fig. 3 and then the virtual leader is placed at the intersection of the sphere and the ray from its center in the direction of the formation movement.

As mentioned in the introduction, we propose to integrate the short term control of the formation and its trajectory planning with the turning maneuvers into a single MPC-based optimization process. In MPC techniques, a finite horizon optimization control problem is solved for the kinematic model of the system from the current states over a time interval (called *control horizon*) with N transition states distributed with constant sampling time Δt. The control inputs are constant in the interval between two consequent transition points. We extend this scheme by another time interval (*planning horizon*) with additional M transition states. The *planning horizon* has the variable time difference between the transition states and it is used for trajectory planning into the desired target region.

The overall trajectory of the formation from its actual state into the target region can be then encoded into a vector of constant control inputs as $X = [v_{v,1},\ v_{h,1},\ \omega_1,\ \alpha_1,\ \dots,\ v_{v,N},\ v_{h,N},\ \omega_N, \alpha_N,\ v_{v,N+1},\ v_{h,N+1},\ \omega_{N+1},\ \delta_{N+1},\ \alpha_{N+1},\ \dots,\ v_{v,N+M},\ v_{h,N+M},\ \omega_{N+M},\ \delta_{N+M},\ \alpha_{N+M}]$, which is used as the optimization vector under the MPC scheme in each planning step. The optimization is frequently restarted from the current state and therefore only the begging of the vector $X^\star$ obtained as result of the optimization is used for MAV control. The vector X consists of the vertical velocity $v_{v,\cdot}$ $[\mathrm{m{\cdot}s^{-1}}]$, the horizontal velocity $v_{h,\cdot}$ $[\mathrm{m{\cdot}s^{-1}}]$, the angular velocity around the vertical axis with origin in the position of the virtual leader $\omega_{\cdot}$ $[\mathrm{rad{\cdot}s^{-1}}]$, the time interval between consequent transition points $\delta_{\cdot}$ $[\mathrm{s}]$, and the angle $\alpha_{\cdot} [rad]$ by which the formation heading is rotated (see Fig. 3 for visualization the rotation maneuver).

Then, we solve trajectory planning and control of the formation as minimization of the cost function $CF(X)$, subject to sets of constraints C_{inputs}, C_{target}, and C_{acc}, such as

$$C_{inputs} := \begin{cases} v_{v,min} \leq v_{v,k} \leq v_{v,max}, \\ |\omega_k| \leq v_{h,k}/R_{min}, \\ if\, \alpha_k = 0,\, 0 \leq v_{h,k} \leq v_{h,max},\, else,\, v_{h,k} = 0, \end{cases} \tag{1}$$

where $k \in \{1 \cdots N + M\}$. The limits $v_{v,min}$ and $v_{v,max}$ are given by the motion capabilities of the MAVs in the formation. The angular velocity is limited by the minimal allowed turning radius R_{min} of the formation that ensures smooth movement of all followers in the desired shape. As shown in [5], R_{min} depends on the size of the formation and it is the main bottleneck of using the L-F technique [5] in a cluttered environment with obstacles, where the limited turning radius decreases maneuverability of the formation. Solving this limitation is the motivation of the proposed migrating virtual leader approach. Also, the limit $v_{h,max}$ depends on the motion capabilities of MAVs and the desired shape of the formation since the robot following the outer track goes faster than the robot closer to the center of the turning if $\omega_k \neq 0$, as described in [5], [18]. The constraint $C_{target} := dist_{target} - r_{target} \leq 0$ ensures that the distance $dist_{target}$ of the last point of the trajectory and the center of the target region is smaller than its radius r_{target}. The set of constraints C_{acc} is defined as

$$C_{acc} := \begin{cases} a_{max} - |v_{h,k+1} - v_{h,k}|/\Delta t \leq 0, k \in 1 \cdots N - 1 \\ a_{max} - |v_{h,k+1} - v_{h,k}|/\delta_k \leq 0, \\ k \in N \cdots N + M - 1, \end{cases} \tag{2}$$

where a_{max} is a limit on the acceleration of the formation in the horizontal plane. Constraints C_{inputs} and C_{acc} are important for integration of the rotating maneuvers into the overall trajectory. These sets ensure that the formation stops before the virtual leader migration, as required for the L-F technique.

The cost function is defined as

$$CF(X) = \min\left\{0, \frac{dist_{obst}(X) - r_s}{dist_{obst}(X) - r_a}\right\}^2 + \sum_{j=N+1}^{N+M} \delta_j$$
$$+ \sum_{j=2}^{N+M} \left((v_{v,j} - v_{v,j-1})^2 + (v_{h,j} - v_{h,j-1})^2 + (\omega_j - \omega_{j-1})^2\right)$$
$$+ \sum_{j=1}^{N+M} ln(|c_1 \cdot \alpha_j| + 1), \qquad (3)$$

where the first term is the obstacle avoidance function originally described in [25], which is zero if the minimal distance $dist_{obst}(X)$ between the trajectory (described by the vector of control inputs X applied on the kinematic model for the actual state) and an obstacle is greater than safety radius r_s and increases if an obstacle approaches into the sphere defined by the safety radius. The spherical representation of the formation is important due to the employed visual relative localization, and it ensures the direct visibility between the followers. The value of the first term of $CF(X)$ goes to infinity as an obstacle approaches the avoidance radius r_a. The time of flight penalization in the second term depends only on the planning horizon since the transition states are distributed with the constant frequency in the control horizon. The third term penalizes movement oscillations, which may occur in MPC control scheme, and it is aimed to prevent the system from an undesired deviation in control inputs. The last term, which penalizes the turning maneuvers, can be used (with its influence set by constant c_1) in applications, where trajectories without the turning maneuver are preferred even at the cost of a longer time to the target. In this paper, a nonzero weight c_1 of this term is used only in the experiment in table I.

B. Stabilization of followers

The desired trajectories for each of the followers are simply obtained from the result of the optimization $X^\star$ using the L-F method from [5] as sketched in section II. As depicted in Fig. 4, the only issue that needs to be considered is the modification of p_i, q_i coordinates after each turning maneuver for all MAVs:

$$p_i = cos(\phi + \alpha)(P_x - P_{ix}) + sin(\phi + \alpha)(P_y - P_{iy}),$$
$$q_i = cos(\phi + \alpha)(P_y - P_{iy}) + sin(\phi + \alpha)(P_x - P_{ix}),$$

where $i \in 1 \cdots N_{MAV}$, $P := [P_x, P_y]$ is the new position of the virtual leader, ϕ is its heading before its migration, and $P_i := [P_{ix}, P_{iy}]$ is position of the i-th follower, which is obtained as $P_i := P_0 + cos(\phi)[-p_i, q_i] - sin(\phi)[q_i, p_i]$. P_0 is position of the virtual leader before its migration. Coordinate h_i stays unchanged during the turning maneuver.

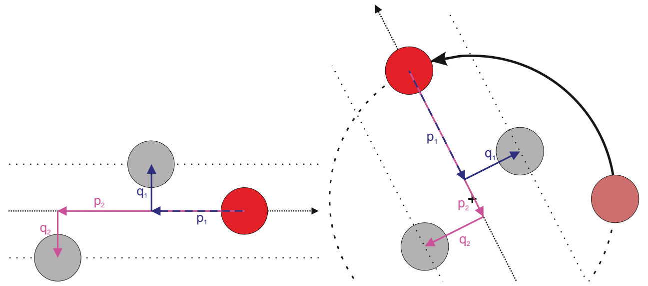

Fig. 4. A formation before (left) and after (right) the virtual leader migration. The virtual leader is represented by the red circle and followers by gray circles.

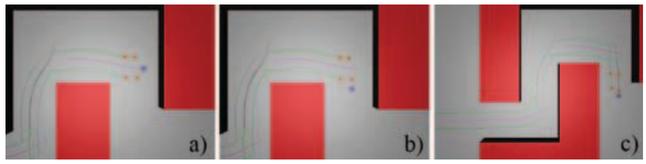

Fig. 5. Formation flying in a narrow corridor, which requires sudden changes of formation velocity to be able to fly around corners without collisions with obstacles and mutual collisions. MAVs are denoted by orange and the virtual leader by blue contours. a) The formation before the third migration of the virtual leader. b) Migration finished. c) Mission accomplished.

The desired trajectories of each MAV can be then directly followed by the onboard embedded MPC solver described in [15]. Unfortunately, the solution in [15] does not include an obstacle avoidance function. If a dynamic environment is considered, inter-vehicle collision avoidance in case of a follower failure is required or the ability to temporarily change the formation shape is needed (as shown in Fig. 6), the algorithm described in section VI.C of our previous work [16] on UGV-formations control needs to be applied in a slower planning loop before employing the fast onboard MPC. Due to the space limit of this paper, we have to skip the description of the extension of the algorithm in [16] for using with MAVs and into 3D, but it is straightforward.

IV. Numerical simulations

In the presented experiments, a C Feasible Sequential Quadratic Programming (CFSQP) library [26] is used for solving the optimization problem defined in III-A. Initial formation parameters in the simulations with snapshots shown in Fig. 5 and 6 and results in table I are $p_i = \{0.5; 0.5; 0.9; 0.9\}$, $q_i = \{0.4; -0.4; 0.4; -0.4\}$, and $r_i = \{0; 0; 0.2; 0.2\}$, while for the simulation in Fig. 8 $p_i = \{0.55; 0.55; 0.3; 0.3; 0.3; 0.3; 0.8; 0.8; 0.8; 0.8\}$, $q_i = \{0; 0; -0.4; -0.4; 0.4; 0.4; 0.4; 0.4; -0.4; -0.4\}$, and $r_i = \{-0.2; 0.2; 0.2; -0.2; 0.2; -0.2; 0.2; -0.2; 0.2; -0.2\}$.

In the first scenario in Fig. 5, the width of the corridor in the workspace does not allow to use the basic L-F approach from [5] and the turning maneuvers with the sudden change of the position of the virtual leader are required. During these turning maneuvers, the formation is forced to stop its movement, the position of the virtual leader is changed, and the formation continues in the new direction.

Fig. 6. Ability of deformation of the formation shape enforced by the narrow passage (a) and avoidance of a lately detected obstacle (b).

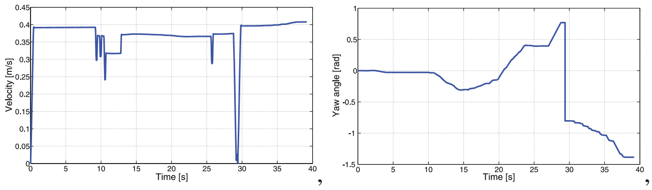

Fig. 7. Progress of velocity (left) and yaw (right) of the virtual leader in the experiment presented in Fig. 6.

In the map in Fig. 6, which is inspired by an office-like environment, the “door” in the first obstacle is smaller than the formation in its desired shape, and the formation has to be temporarily narrowed there to be able to pass through. A response of the formation to lately detected obstacle is demonstrated by the straight obstacle inside the room, which is considered as unknown at the beginning of the simulation. The turning maneuver at the end of the experiment (see the yaw and velocity profiles in Fig. 7 shortly before the 30th second of the simulation) is not necessary due to the environment constraints, but this solution is evaluated by a cheaper cost value than a longer solution without the maneuver. The temporary decrease of speed of the formation motion between the 9. and 13. second of the simulation is caused by the later detected obstacle.

In the simulation in Fig. 8, the system scalability is tested using the 10-MAVs formation. The progress of cost function values of solutions obtained in each planning step is shown in Fig. 9. The cost is linearly decreasing due to the constant speed of the formation movement (the trajectory is shortened by the approximately same distance in each planning step), except the intervals along the displacement of the virtual leader position, where the decrease of cost values is faster. The progress of heading direction of the virtual leader during the simulation is shown in Fig. 9. The airflow influence of the top MAVs to the bottom MAVs, which is observed in real-world experiments, is neglected in this simulation. This enables us to verify the ability of the system to stabilize large compact formations of 3D shape. Real-world applicability of such a compact 3D formation would be possible only with smaller MAVs (as shown in [27]) than using the platforms considered in this paper.

The influence of weight of penalization of the rotation maneuvers c_1 in the cost function (3) is shown in table I. The aim of this statistic, which was obtained by 2100 simulations in 300 randomly generated scenarios (see examples of the scenarios in Fig. 10), is to verify the reliability of the method and its ability to choose between smooth longer trajectories and shorter trajectories with included turning maneuvers based on

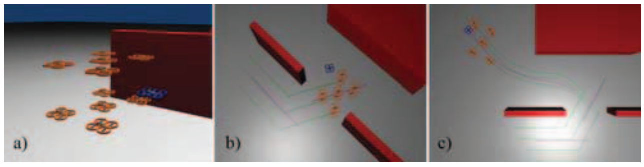

Fig. 8. A formation of 10 MAVs flying in a narrow corridor. Airflow effect from MAV propellers to neighboring vehicles was not considered in this simulation. a) Initial position. b) The formation after the second migration. c) Target reached.

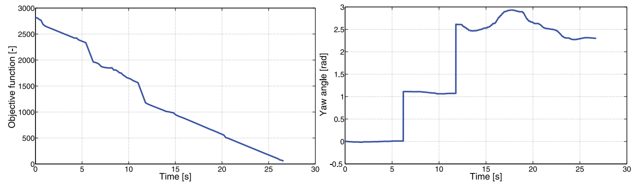

Fig. 9. Progress of cost function values of solutions of the virtual leader motion planning problem (left) and yaw (right) of the virtual leader in the simulation with snapshots presented in Fig. 8.

the particular application. In the table, the trajectory curvature value is obtained as mean curvature along the 300 trajectories followed by the formation. The flight time is the mean total time of flight to reach the desired target location and the minimum obstacle distance is mean minimal distance between an MAV and an obstacle in the 300 runs of the algorithm for each setting of weight c_1.

Results of this analysis are also displayed as a box plot in Fig. 11, where the red line represents the median and edges of the blue rectangle are the 25-th and 75-th percentiles. The whiskers are extended to the most extreme data points that are not considered as outliers, which are plotted individually as the red crosses. Points are considered as outliers if they are larger than $q_3 + w(q_3 - q_1)$ or smaller than $q_1 - w(q_3 - q_1)$, where q_1 and q_3 are the 25-th and 75-th percentiles, respectively, and w is the whisker length.

Results confirmed that the number of turning maneuvers (counted in the first three rows of the table) significantly decreases with increasing value of the weight of penalization of these maneuvers in the cost function. With the increasing number of the turning maneuvers, the curvature of the obtained trajectories increases and also the minimal distance between the formation and obstacles decreases if the trajectories without turning maneuvers are preferred, which both increase flight safeness. This shows the usefulness of the method in cluttered

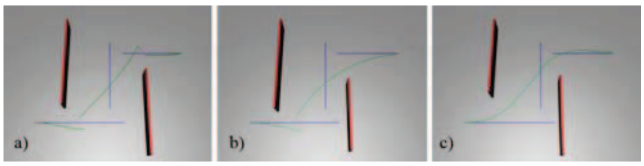

Fig. 10. Examples of solutions of different scenarios found by the proposed algorithm in the statistics presented in Fig. 11 and table I. The initial trajectory is plotted in blue, obtained trajectories in green and obstacles in red color. a) A solution with 2 maneuvers, b) with 1 maneuver, c) without a maneuver.

weight	0	25	50	75	150	300	1000
2 manoeuvres	299	257	194	140	109	92	38
1 manoeuvre	1	38	85	129	150	151	175
0 manoeuvres	0	5	21	31	41	57	87
min. obst. dist.	1.25	1.24	1.23	1.22	1.19	1.16	1.09
traj. curvature	2.56	3.08	3.47	3.89	4.17	4.43	5.04

TABLE I

INFLUENCE OF THE WEIGHT c_1 OF THE TERM IN THE COST FUNCTION (3) THAT PENALIZES THE ROTATION MANEUVERS IN THE SOLUTION. EACH SETTING OF THE PARAMETER c_1 WAS TESTED IN 300 SIMULATIONS OF RANDOMLY GENERATED SCENARIOS.

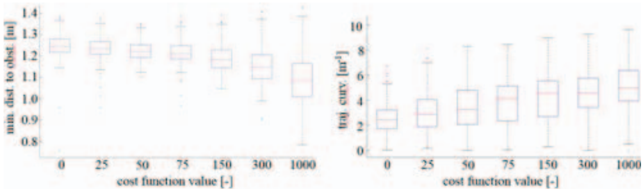

Fig. 11. Minimal distance to obstacles (a) and curvature of the trajectory (b) of solutions obtained by the algorithm with different setting of the parameter c_1. Each statistic was obtained from 300 simulations of randomly generated scenarios.

environments, additionally to the ability to solve situations, where a feasible trajectory does not exist if the turning maneuvers are not enabled, as was shown in the previous simulations.

V. CONCLUSION

In this paper, a novel concept of motion planning and stabilization of formations of micro aerial vehicles based on a dynamic virtual leader was designed and experimentally evaluated. This concept is suited for utilization of onboard visual relative localization of neighboring MAVs, which can be considered as an enabling technique for deployment of large teams of unmanned helicopters in cluttered and GPS-denied environments. The results of theoretical analyzes of system stability and convergence of the MPC-based planning and results of the numerical simulations show that the proposed method is capable of flexible formation flying in cluttered GPS-denied environments and it is robust to external disturbances caused by the wind, air turbulence close to walls, and imprecise sensors.

ACKNOWLEDGMENT

The work has been supported by contract with Khalifa University of Science via CTU HS No. 13167/830/8301616C, by MSMT under grant No. 7AMB16FR017, and by GACR via grant No. 16-24206S.

REFERENCES

[1] T. Krajnik, M. Nitsche, J. Faigl, P. Vanek, M. Saska, L. Preucil, T. Duckett, and M. Mejail, "A practical multirobot localization system," *Journal of Intelligent & Robotic Systems*, vol. 76, pp. 539–562, 2014.

[2] J. Faigl, T. Krajník, , J. Chudoba, L. Preucil, and M. Saska, "Low-cost embedded system for relative localization in robotic swarms," in *IEEE ICRA*, 2013.

[3] Y. Zhang and K. Ma, "Lighting design for globally illuminated volume rendering." *IEEE Transactions on Visualization and Computer Graphics*, vol. 19, pp. 2946–55, 2013.

[4] G. Droge, "Distributed virtual leader moving formation control using behavior-based mpc," in *ACC*, 2015.

[5] T. D. Barfoot and C. M. Clark, "Motion planning for formations of mobile robots," *Robotics and Auton. Syst.*, vol. 46, pp. 65–78, 2004.

[6] J. wook Kwon, J. H. Kim, and J. Seo, "Article multiple leader candidate and competitive position allocation for robust formation against member robot faults," *Sensors*, vol. 15, no. 5, pp. 10 771–10 790, 2015.

[7] S. Swaminathan, M. Phillips, and M. Likhachev, "Planning for multi-agent teams with leader switching," in *IEEE ICRA*, 2015.

[8] P. A. Sperandio Giacomin and E. M. Hemerly, "Reconfiguration between longitudinal and circular formations for multi-uav systems by using segments," *Journal of Intelligent & Robotic Systems*, vol. 78, no. 2, pp. 339–355, 2014.

[9] O. Cetin and G. Yilmaz, "Real-time autonomous uav formation flight with collision and obstacle avoidance in unknown environment," *Journal of Intelligent & Robotic Systems*, pp. 1–19, 2016.

[10] K. A. Ghamry and Y. Zhang, "Formation control of multiple quadrotors based on leader-follower method," in *ICUAS*, 2015.

[11] A. Monteriu, "Nonlinear decentralized model predictive control for unmanned vehicles moving in formation," *Information Technology and Control*, vol. 44, no. 1, pp. 89–97, 2015.

[12] S. Garrido, L. Moreno, and P. U. Lima, "Robot formation motion planning using fast marching," *Robotics and Autonomous Systems*, vol. 59, no. 9, pp. 675 – 683, 2011.

[13] C. Papachristos, K. Alexis, and A. Tzes, "Model predictive hovering-translation control of an unmanned tri-tiltrotor," in *IEEE ICRA*, 2013.

[14] K. Alexis, C. Papachristos, R. Siegwart, and A. Tzes, "Robust explicit model predictive flight control of unmanned rotorcrafts: Design and experimental evaluation," in *ECC*, 2014.

[15] T. Baca, G. Loianno, and M. Saska, "Embedded model predictive control of unmanned micro aerial vehicles," in *MMAR*, 2016.

[16] M. Saska, V. Spurny, and V. Vonasek, "Predictive control and stabilization of nonholonomic formations with integrated spline-path planning," *Robotics and Autonomous Systems*, vol. 75, no. B, pp. 379–397, 2016.

[17] M. Saska, V. Vonasek, and L. Preucil, "Trajectory Planning and Control for Airport Snow Sweeping by Autonomous Formations of Ploughs," *Journal of Intelligent and Robotic Systems*, vol. 72, no. 2, pp. 239–261, 2013.

[18] M. Saska, V. Vonasek, T. Krajnik, and L. Preucil, "Coordination and Navigation of Heterogeneous MAV&UGV Formations Localized by a "hawk-eye"-like Approach Under a Model Predictive Control Scheme," *International Journal of Robotics Research*, vol. 33, no. 10, pp. 1393–1412, September 2014.

[19] M. Saska, T. Krajnik, V. Vonasek, Z. Kasl, V. Spurny, and L. Preucil, "Fault-Tolerant Formation Driving Mechanism Designed for Heterogeneous MAVs-UGVs Groups," *Journal of Intelligent and Robotic Systems*, vol. 73, no. 1-4, pp. 603–622, 2014.

[20] M. Saska, V. Vonasek, and L. Preucil, "Roads Sweeping by Unmanned Multi-vehicle Formations," in *IEEE ICRA*, 2011.

[21] V. Spurny, T. Baca, and M. Saska, "Complex manoeuvres of heterogeneous mav-ugv formations using a model predictive control," in *MMAR*, 2016.

[22] D. J. E.G Gilbert and S. Keerthi, "A fast procedure for computing the distance between complex objects in three-dimensional space," *Robotics and Automation, IEEE Journal of*, vol. 4, no. 2, pp. 193 – 203, 1988.

[23] D. Scaramuzza and at al., "Vision-controlled micro flying robots: From system design to autonomous navigation and mapping in gps-denied environments," *IEEE Robotics Automation Magazine*, vol. 21, no. 3, pp. 26–40, 2014.

[24] M. Saska, J. Mejia, D. Stipanovic, V. Vonasek, K. Schilling, and L. Preucil, "Control and Navigation in Manoeuvres of Formations of Unmanned Mobile Vehicles," *European Journal of Control*, vol. 19, no. 2, pp. 157–171, March 2013.

[25] D. M. Stipanović, P. F. Hokayem, M. W. Spong, and D. D. Šiljak, "Cooperative avoidance control for multi-agent systems," *Journal of Dynamic Systems, Measurement, and Control*, vol. 129, pp. 699–707, 2007.

[26] J. Z. C. Lawrence and A. Tits, "User's guide for cfsqp version 2.5," University of Maryland, 1997.

[27] A. Kushleyev, D. Mellinger, C. Powers, and V. Kumar, "Towards a swarm of agile micro quadrotors," *Autonomous Robots*, vol. 35, no. 4, pp. 287–300, 2013.